Supplemental material to this article can be found at:
http://molpharm.aspetjournals.org/content/suppl/2022/09/27/molpharm.122.000539.DC2
1521-0111/102/6/248–258$35.00 http://molpharm.aspetjournals.org/content/suppl/2022/09/24/molpharm.122.000539.DC1 https://doi.org/10.1124/molpharm.122.000539
MOLECULAR PHARMACOLOGY Mol Pharmacol 102:248–258, December 2022

Cancer-Type Organic Anion Transporting Polypeptide 1B3 Is Localized in Lysosomes and Mediates Resistance against Kinase Inhibitors[S]

Bastian Haberkorn, Stefan Oswald, Niklas Kehl, Arne Gessner, R. Verena Taudte, Jan Philipp Dobert, Friederike Zunke, Martin F. Fromm, and Jörg König

Institute of Experimental and Clinical Pharmacology and Toxicology (B.H., N.K., A.G., R.V.T., M.F.F., J.K.) and Department of Molecular Neurology, University Hospital (J.P.D., F.Z.), Friedrich-Alexander-Universität Erlangen-Nürnberg, Erlangen, Germany; and Institute of Toxicology and Pharmacology, Rostock University Medical Center, Rostock, Germany (S.O.)

Received April 8, 2022; accepted September 5, 2022

ABSTRACT

Cancer-type organic anion transporting polypeptide 1B3 (Ct-OATP1B3), a splice variant of the hepatic uptake transporter OATP1B3 (liver-type), is expressed in several tumor entities, including colorectal carcinoma (CRC) and breast cancer. In CRC, high OATP1B3 expression has been associated with reduced progression-free and overall survival. Several kinase inhibitors used for antitumor treatment are substrates and/or inhibitors of OATP1B3 (e.g., encorafenib, vemurafenib). The functional importance of Ct-OATP1B3 has not been elucidated so far. Human embryonic kidney 293 cells stably overexpressing Ct-OATP1B3 protein were established and compared with control cells. Confocal laser scanning microscopy, immunoblot, and proteomics-based expression analysis demonstrated that Ct-OATP1B3 protein is intracellularly localized in lysosomes of stably transfected cells. Cytotoxicity experiments showed that cells recombinantly expressing the Ct-OATP1B3 protein were more resistant against the kinase inhibitor encorafenib compared with control cells [e.g., encorafenib (100 μM) survival rates: 89.5% versus 52.8%]. In line with these findings, colorectal cancer DLD1 cells endogenously expressing Ct-OATP1B3 protein had poorer survival rates when the OATP1B3 substrate bromosulfophthalein (BSP) was coincubated with encorafenib or vemurafenib compared with the incubation with the kinase inhibitor alone. This indicates a competitive inhibition of Ct-OATP1B3–mediated uptake into lysosomes by BSP. Accordingly, mass spectrometry-based drug analysis of lysosomes showed a reduced lysosomal accumulation of encorafenib in DLD1 cells additionally exposed to BSP. These results demonstrate that Ct-OATP1B3 protein is localized in the lysosomal membrane and can mediate transport of certain kinase inhibitors into lysosomes, revealing a new mechanism of resistance.

SIGNIFICANCE STATEMENT

This study describes the characterization of a tumor-associated splice variant (cancer-type organic anion transporting polypeptide; Ct-OATP1B3) of the liver-type OATP1B3 protein (Lt-OATP1B3). This variant is localized in lysosomes mediating resistance against kinase inhibitors that are substrates of this transport protein by transporting them into lysosomes and thereby reducing the cytoplasmic concentrations of these drugs. Therefore, the expression of the cancer-type OATP1B3 protein is associated with a better survival of cells, revealing a new mechanism of drug resistance.

Introduction

Transport proteins are important for the uptake, distribution, and excretion of xenobiotics, drugs, and endogenous substances in normal and cancerous tissues (Robey et al., 2018; Pizzagalli et al., 2021). Export proteins usually belong to the superfamily of ABC (ATP-binding cassette) transporters (Moitra and Dean, 2011; Locher, 2016), whereas uptake transporters are members of the SLC (solute carrier) transporter superfamily (Pizzagalli et al., 2021). Additional to their expression in all healthy tissues, including intestine, kidney, and liver, ABC and SLC transporters are also expressed in several cancerous tissues mediating the uptake or export of drugs or endogenous substrates into or out of cancer cells (Robey et al., 2018; Al-Abdulla et al., 2019; Zhang and Wang, 2020). Remarkably, during antitumor therapy, ABC transporters in particular have been characterized as important mediators of drug resistance when they are overexpressed in cancerous tissues (Robey et al., 2018), whereas in this

This work was supported by the Wilhelm Sander-Stiftung (Grants 2019.050.1 and 2019.097.1) and by the DFG (Grant INST 90/1048-1 FUGG).
The authors declare no conflict of interest.
dx.doi.org/10.1124/molpharm.122.000539.
[S] This article has supplemental material available at molpharm.aspetjournals.org.

ABBREVIATIONS: ABC, ATP-binding cassette; BSP, bromosulfophthalein; CRC, colorectal carcinoma; Ct-OATP1B3, cancer-type organic anion transporting polypeptide 1B3; $E_2$17βG, estradiol-17β-glucuronide; HEK293, human embryonic kidney 293; LAMP1, lysosomal-associated membrane protein 1; Lt-OATP1B3, liver-type organic anion transporting polypeptide 1B3; OATP1B3, organic anion transporting polypeptide 1B3; OG, Oregon Green 488 carboxylic acid, succinimidyl ester; OICE, Optical Imaging Center Erlangen; SLC, solute carrier; VC, vector control.

context, the role of SLC transporters is currently under intensive investigation (Neul et al., 2016; Huang et al., 2020; Krchniakova et al., 2020; Sun et al., 2020).

The focus of this study is on a variant of the SLCO/SLC21 family member organic anion transporting polypeptide 1B3 (OATP1B3, gene symbol *SLCO1B3*). OATP1B3 has been characterized as an uptake transporter predominantly localized in the basolateral membrane of human hepatocytes (König et al., 2000). Several endogenous substances as well as widely prescribed drugs have been identified as substrates of this transporter (Seithel et al., 2008; Fahrmayr et al., 2010; Roth et al., 2012). Transported drugs include 3-hydroxy-3-methylglutaryl-coenzyme A reductase inhibitors (statins), antibiotics, and several antitumor therapeutic agents such as methotrexate, paclitaxel, and kinase inhibitors (e.g., vemurafenib) (Zimmerman et al., 2013; Kayesh et al., 2021).

In 2001, Abe et al. (2001) reported that OATP1B3 is also expressed in several cancerous tissues and cancer-derived cells. Nagai et al. (2012) finally demonstrated that not the liver-type OATP1B3 protein (Lt-OATP1B3) but an isoform of the Lt-OATP1B3 protein termed cancer-type OATP1B3 protein (Ct-OATP1B3) is expressed in human cancerous tissues. This isoform results from alternative splicing of the *SLCO1B3* gene with the *Ct-SLCO1B3* mRNA possessing a unique first exon (called exon 1*), which originates from an alternative transcriptional start site located in intron 3 (Fig. 1a) of the *SLCO1B3* gene (Nagai et al., 2012). Ct-OATP1B3 protein encoded by the alternatively spliced *Ct-SLCO1B3* mRNA lacks the first 28 amino acids of Lt-OATP1B3 [Fig. 1b (Sun et al., 2014)]. Sun et al. (2014) could discriminate between *Lt-* and *Ct-SLCO1B3* mRNA and demonstrated that *Ct-SLCO1B3* mRNA is expressed in 87.2% of investigated colorectal cancer tissues but only in 2.6% of the adjacent healthy tissues. So far, in vitro data regarding Ct-OATP1B3 protein transport function and subcellular localization are controversial (Imai et al., 2013; Thakkar et al., 2013; Sun et al., 2014). Interestingly, it has been demonstrated that the aminoterminal region of the OATP1B3 protein, which is present in Lt-OATP1B3 but absent in Ct-OATP1B3 (Fig. 1C), seems to be important for the correct insertion of Lt-OATP1B3 in the plasma membrane (Chun et al., 2017).

Expression of *Ct-SLCO1B3* mRNA or Ct-OATP1B3 protein has been confirmed in different cancerous tissues, including colorectal (Abe et al., 2001; Lee et al., 2008), gastric (Abe et al., 2001), breast (Muto et al., 2007), prostate (Hamada et al., 2008; Pressler et al., 2011), and pancreatic cancer (Kounnis et al., 2011; Hays et al., 2013). Interestingly, a study with 278 colorectal tumor samples demonstrated a higher *Ct-SLCO1B3* mRNA expression in lower stage tumors (Lockhart et al., 2008), whereas Lee et al. (2008) found no correlation between tumor stage and *Ct-SLCO1B3* mRNA expression. Furthermore, some studies found that a high expression of Ct-OATP1B3 protein is associated with a better overall survival of colorectal cancer or endometrial cancer patients (Lockhart et al., 2008; Ogane et al., 2013; Tang et al., 2021), whereas other studies found that a high expression of *Ct-SLCO1B3* mRNA is associated with a reduced progression-free survival in patients with advanced and metastatic colorectal cancer (Teft et al., 2015). Recently, a high *SLCO1B3* gene expression was associated with lower overall survival in patients with colorectal cancer (Zhi et al., 2021). Taken together, the cancer-type variant of OATP1B3 protein is expressed in several cancerous tissues, but the localization, transport function, and possible role of expression needs to be elucidated. Therefore, the aim of this exploratory study is to gain insights into the subcellular localization, transport function, and possible functional role of Ct-OATP1B3.

Materials and Methods

Materials. [^{3}H]-bromosulfophthalein (BSP, 14 Ci/mmol) was obtained from HARTMANN ANALYTIK GmbH (Braunschweig, Germany). [^{3}H]-estradiol-17β-glucuronide ($E_2$17βG, 50 Ci/mmol) was purchased from American Radiolabeled Chemicals, Inc. (St. Louis, MO). Stably labeled [$^2H_3$]-clopidogrel was purchased from

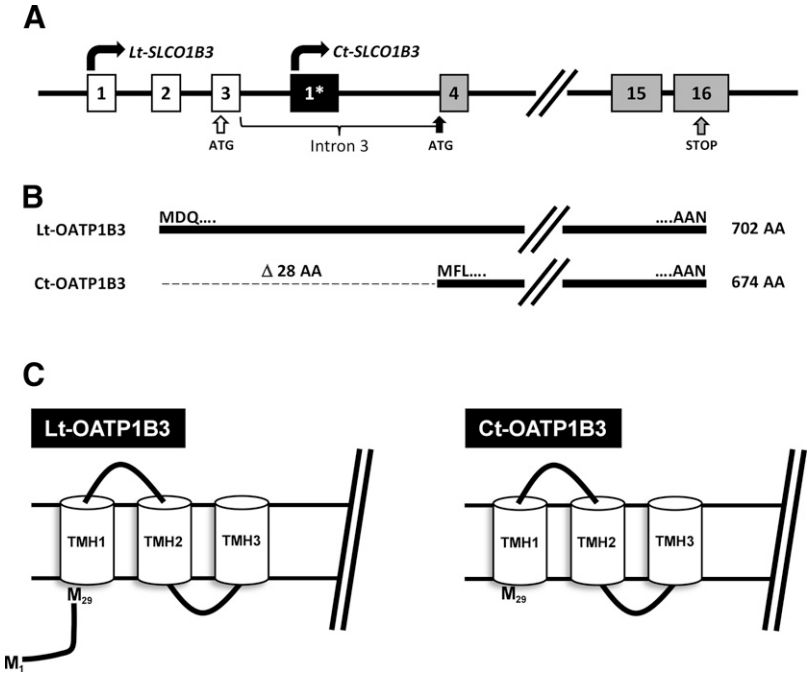

Fig. 1. Structure of the *SLCO1B3* gene and the encoded two protein variants. (A) Structure of the human *SLCO1B3* gene. The transcriptional start sides of both variants (*Lt-SLCO1B3* and *Ct-SLCO1B3*) are indicated with curved arrows. The white boxes representing the first three exons of the *Lt-SLCO1B3* variant lacking in the *Ct-SLCO1B3* variant. The black box indicates exon 1* within intron 3 of the *SLCO1B3* gene, which is alternatively spliced in front of exon 4 of the *Lt-SLCO1B3* gene. Exons 4–16 (gray boxes) are identical for the *Lt-* and *Ct-SLCO1B3* gene variants. Both start codons (ATG) are depicted below the gene structure; ATG in exon 3 is the start codon for the Lt-OATP1B3 protein, and ATG at the beginning of exon 4 is the start codon for the Ct-OATP1B3 protein. The stop codon located in exon 16 is identical for both variants. The gene bank entry NM_019844.4 served as reference sequence for the *Lt-SLCO1B3* mRNA and the gene bank entry NM_001349920.2 for the *Ct-SLCO1B3* mRNA. (B) Proteins encoded by both gene variants with the Ct-OATP1B3 protein lacking the first 28 amino acids of the Lt-OATP1B3 protein. (C) Schematic two-dimensional overview over the aminoterminal regions of Lt- and Ct-OATP1B3 predicted by DeepTMHMM-Predictions. AA, amino acids; MDQ, first three amino acids of the Lt-OATP1B3 protein; MFL, first three amino acids of the Ct-OATP1B3 protein; AAN, last three amino acids of both OATP proteins; TMH, transmembrane helix.

@rtMolecule (Poitiers, France). Unlabeled BSP was from AppliChem GmbH (Darmstadt, Germany); unlabeled $E_2 17\beta G$ and the ProteoExtract Native Membrane Protein Extraction Kit were from Sigma Aldrich (St. Louis, MO). Regorafenib was purchased from LC Laboratories (Woburn, MA). Encorafenib and vemurafenib were from MedChemtronica AB (Sollentuna, Sweden). Minimum essential medium, Dulbecco's modified Eagle's medium/F12(1:1), RPMI 1640, Dulbecco's phosphate buffered saline, fetal bovine serum, hygromycin B (50 mg/mL), penicillin streptomycin solution, 0.05%-trypsin-EDTA solution, Pierce BCA Protein Assay Kit, CellLight Lysosomes-RFP, BacMam 2.0, and the SYTOX Green nucleic acid stain were obtained from Thermo Fisher Scientific (Dreieich, Germany). The NucleoSpin RNA Plus Kit was obtained from MACHEREY-NAGEL GmbH & Co. KG (Düren, Germany). The iScript cDNA Synthesis Kit was from Bio-Rad Laboratories GmbH (München, Germany). The Minute Plasma Membrane Protein Isolation and Cell Fractionation Kit was purchased from Invent Biotechnologies, Inc. (Plymouth, MN). Six-well, 12-well, and 96-well cell culture plates were from Greiner Bio-One (Frickenhausen, Germany). Oregon Green 488 carboxylic acid, succinimidyl ester (OG) was obtained from Invitrogen (Rockford, IL). The LightCycler FastStart DNA Master^{PLUS} SYBR Green I Kit was obtained from Roche Diagnostics GmbH (Mannheim, Germany). SPY555-DNA (SPY dyes series) was from Spirochrome AG (Stein am Rhein, Switzerland), and the pmScarlet-1_peroxisome_C1 plasmid (RRID:Addgene_85065; Addgene, Watertown, MA) was kindly provided by the Optical Imaging Center Erlangen (OICE). The μ-Slide 8-well glass bottom arrays were obtained by ibidi GmbH (Gräfeling, Germany). The CCK-8 Assay was purchased from GERBU Biotechnik GmbH (Heidelberg, Germany).

Antibodies. Polyclonal rabbit anti–human OATP1B3 antiserum (SKT, indicating the first three amino acids of the epitope: serine, lysine and threonine) directed against the carboxyterminal end of the human OATP1B3 protein (König et al., 2000) was obtained from the Division of Tumor Biochemistry of the German Cancer Research Center (Heidelberg, Germany). The goat anti–rabbit IgG horseradish peroxidase–labeled antibody (RRID:AB_2650489) was purchased from GE Healthcare Life Sciences (Buckinghamshire, UK). The goat anti–mouse IgG Alexa Fluor Plus 647 antibody (RRID:AB_2633277), the Alexa Fluor 568 goat anti–rabbit IgG antibody (RRID:AB_143157), the goat anti–mouse IgG (H+L) secondary antibody, and the HRP antibody (RRID:AB_2533947) were from Thermo Fisher Scientific (Dreieich, Germany). The Anti–alpha 1 Sodium Potassium ATPase antibody (RRID:AB_306023) was from Abcam plc. (Cambridge, UK). The monoclonal mouse anti–pan cadherin antibody (RRID:AB_476826), the mouse anti–β-actin monoclonal antibody (RRID:AB_476743), and the anti–lysosomal-associated membrane protein 1 (LAMP1) antibody produced in rabbit (RRID:AB_477157) were purchased from Sigma-Aldrich (St. Louis, MO).

Cell Culture. Human embryonic kidney 293 (HEK293; RRID: CVCL_0045) cells were obtained from the American Type Culture Collection and incubated at 37 °C and 5% CO_2. The cell culture medium was minimum essential medium, supplemented with 10% heat-inactivated fetal bovine serum, 100 U/mL penicillin, and 100 μg/mL streptomycin. For antibiotic selection, hygromycin B (250 μg/mL) was added. The stable-transfected cell lines were routinely checked for expression of the respective transport protein. DLD1 (RRID:CVCL_0248) and T84 cells (RRID:CVCL_0555) were kindly provided by Dr. Britzen-Laurent and Dr. Naschberger (Department of Surgery, Erlangen, Germany). All human cell lines have been authenticated using Short Tandem Repeat (or single-nucleotide polymorphism) profiling within the last 3 years, and the experiments were performed with mycoplasma-free cells. For DLD1 cells, RPMI 1640 medium was used, and for T84 cells, Dulbecco's modified Eagle's medium/F12 (1:1) was used, both supplemented with 10% heat-inactivated fetal bovine serum, 100 U/mL penicillin, and 100 μg/mL streptomycin. Subcultivation was done twice a week using trypsin 0.05%–EDTA 0.02% solution.

Generation of Stably Transfected HEK-Ct-OATP1B3 and HEK-Kz-Ct-OATP1B3 Cells. For the amplification of the *Ct-SLCO1B3* cDNA, synthesized single-stranded cDNA of human colon tumor total RNA served as template, using oCt-OATP1B3-5′-For (5′-aactgcagatgttcttggcag-3′) and oOATP1B3-RT-Rev2 (5′-gcatagacttatccattggtcc-3′) as primers. Subsequent to TOPO-TA cloning, the *Ct-SLCO1B3* cDNA was cloned into the expression vector pcDNA3.1 Hygro(-), resulting in the plasmid pCt-SLCO1B3.31_Hygro. To introduce the Kozak sequence around the start ATG, the pCt-SLCO1B3.31_Hygro plasmid and the primer pair oCt-OATP1B3.Kozak.For (5′-gccgccaccatgttcttggcagc-3′) and oOATP1B3-RT-Rev2 were used to amplify a modified cDNA. This cDNA was cloned into the vector pcR2.1.Topo and subcloned into the expression vector pcDNA3.1 Hygro(-), resulting in the plasmid pKozak-Ct-SLCO1B3.31_Hygro. Before transfection, all cDNAs were sequenced, and both plasmids contain a cDNA encoding the same Ct-OATP1B3 protein. Stable transfectants expressing the Ct-OATP1B3 protein were established in the same way as described before by Taghikhani et al. (2019), resulting in the HEK293 cell lines HEK-Ct-OATP1B3 and HEK-Kz-Ct-OATP1B3.

Quantitative Polymerase Chain Reaction. Total RNA was isolated using the NucleoSpin RNA Plus Kit according to the manufacturer's protocol. The concentration of the isolated RNA was photometricly measured. The iScript cDNA Synthesis Kit was used according to the manufacturer's protocol to generate the first-strand cDNA using 1 μg total RNA per sample. For the quantitative reverse transcriptase PCR reaction, the LightCycler FastStart DNA Master^{PLUS} SYBR Green I Kit was used. Each sample consisted of 5 μL purified water, 2 μL solution I (Kit included), 1 μL forward and reverse primer, respectively, and 1 μL template single-stranded cDNA. Subsequent to the initial 10-minute denaturation step at 95 °C, the DNA was amplified during 45 cycles of 10-second denaturation at 95 °C, 10-second annealing at 64 °C, and 30-second elongation at 72 °C. The expression of each sample was calculated via linear regression and normalized to the respective expression of the housekeeping gene *β-actin*.

Immunoblot Analysis. The immunoblot analysis was performed as described earlier (Taghikhani et al., 2020). A protein amount of 30 μg was used for the whole cell homogenate. The plasma membrane fractions and cytosolic fractions were adjusted to an amount of 10 μg protein. For the detection of the OATP1B3 protein, the membrane was incubated with the polyclonal antiserum SKT (1:500) at 4 °C overnight. To detect the binding of the primary antibody, the goat anti–rabbit IgG horseradish peroxidase–labeled antibody (1:10 000) served as secondary antibody. To control sample loading, either the monoclonal mouse anti–human β-actin primary antibody (1:10,000) or the monoclonal mouse anti–pan cadherin antibody (1:2,000) was used. The goat anti–mouse IgG horseradish peroxidase–labeled antibody (1:2,000) was used as secondary antibody. For the analysis of the enriched lysosomal fraction, 10 μg protein was used and staining with the rabbit anti–LAMP1 antibody (1:1,000) served as loading control.

Immunofluorescence Microscopy. Cells were seeded at an initial cell number of 3×10^5 cells per well on poly-D-lysine–coated object slides. After 24 hours, cells were fixed using 70% ice-cold methanol solution and permeabilized with 0.4% Triton X-100 PBS solution. To block the fixed cells, 2% bovine serum albumin solution was added, and the cells were incubated with the polyclonal antiserum SKT (1:500) and the Anti–alpha 1 Sodium Potassium ATPase antibody (1:500) overnight at 4 °C. Alexa Fluor 568 antibody and Alexa Fluor Plus 647 antibody were used as secondary antibodies (1:2000). The nuclei were counterstained with SYTOX Green nucleic acid stain. Microscopy was performed on the Zeiss Spinning Disc Axio Observer Z1 at the OICE (Erlangen, Germany).

Subcellular Fractionation. To separate the plasma membrane fraction from the cytosolic fraction of the stable transfectants, 1×10^7 cells were seeded on 10 cm plates. Twenty-four hours later, protein expression was induced with the addition of sodium butyrate (final concentration 10 mM). Forty-eight hours after seeding, cells were washed with 2 mL PBS, and after the addition of 1.5 mL PBS, cells were transferred into a 2 mL microcentrifuge tube and centrifuged

for 5 minutes at 600 *g* at 4 °C. For isolation, the Minute Plasma Membrane Protein Isolation and Cell Fractionation kit was used. The plasma membrane fraction was finally dissolved in 50 μL of the extraction buffer II of the ProteoExtract Native Membrane Protein Extraction kit. For immunoblot analysis, the plasma membrane fraction was lysed in 0.2% SDS solution containing the complete Tablets (Roche Diagnostics GmbH, Mannheim, Germany) as proteinase inhibitor cocktail.

Lysosome Enrichment. The lysosome fraction was isolated according to Mazzulli et al. (2011). For each sample, cells from three 10 cm plates (1×10^7 cells per plate) were pooled and resuspended in 600 μL sucrose-HEPES buffer (0.25 M sucrose, 10 mM HEPES pH 7.4, 0.1 M EDTA). The cell suspension was homogenized using the B.Braun Potter S homogenizer and subsequently centrifuged for 5 minutes at 6,800 *g* and 4 °C. The supernatant was saved, and the pellet was again resuspended in 600 μL sucrose-HEPES buffer, and homogenization and centrifugation were repeated. Both supernatants were combined and centrifuged for 10 minutes at 17,000 *g* and 4 °C. The supernatant was removed, and the pellet, containing the enriched lysosomal fraction, was saved until further use. For immunoblot analysis, the final pellet was lysed in 0.2% SDS solution containing proteinase inhibitor cocktail.

Protein Quantification by liquid chromatography tandem mass spectrometry. Protein abundance of OATP1B3 and Na/K-ATPase as reference protein was determined using a validated liquid chromatography tandem mass spectrometry-based targeted proteomics assay as described elsewhere (Drozdzik et al., 2019). To isolate the crude membrane protein fraction, the cell pellets from five 75 cm^2 cell culture flasks per sample were pooled and isolated with the ProteoExtract Native Membrane Protein Extraction kit (Merck KGaA, Darmstadt, Germany) according to the manufacturer's protocol. The protein concentration of the obtained crude membrane fractions was determined with the BCA assay. To analyze the amount of OATP1B3 protein in the plasma membrane fraction, the Minute Plasma Membrane Protein Isolation and Cell Fractionation kit was used as mentioned above. If necessary, membrane fractions were adjusted to a maximum protein amount of 2 mg/mL.

Subsequently, 100 μL of each membrane fraction was mixed with 10 μL dithiothreitol (200 mM; Sigma-Aldrich, Taufkirchen, Germany), 40 μL ammonium bicarbonate buffer (50 mM, pH 7.8; Sigma-Aldrich, Taufkirchen, Germany), and 10 μL ProteaseMAX (1% m/v; Promega, Mannheim, Germany) and incubated for 20 minutes at 60 °C (denaturation).After cooling down, 10 μL iodoacetamide (400 mM; Sigma-Aldrich, Taufkirchen, Germany) was added, and the samples were incubated in a darkened water quench for 15 minutes at 37 °C (alkylation). For protein digestion, 10 μL trypsin (trypsin:protein ratio: 1:40; Promega, Mannheim, Germany) was added, and samples were incubated in a water quench for 16 hours at 37 °C. Digestion was stopped by the addition of 20 μL formic acid (10% v/v; Sigma-Aldrich, Taufkirchen, Germany). All samples were stored at −80 °C until further processing. The samples were centrifuged one more time for 15 minutes at 16,000*g* and 4 °C. Finally, 50 μL of the supernatant was mixed with 25 μL isotope-labeled internal standard peptide mix (10 nM of each internal standard; Thermo Fisher Scientific, Dreieich, Germany). All sample preparations and digestion steps were performed using Protein LoBind tubes (Eppendorf, Hamburg, Germany). Protein quantification was conducted on a 5500 QTRAP triple quadrupole mass spectrometer (AB Sciex, Darmstadt, Germany) coupled to an Agilent Technologies 1260 Infinity system (Agilent Technologies, Waldbronn, Germany) using validated liquid chromatography tandem mass spectrometry methods as recently described (Gröer et al., 2013). The monitored peptides for OATP1B3 were ISITQIER, IYNSVFFGR, and NVTGFFQSLK, whereas LSLDELHR was used for Na/K-ATPase. For each peptide, 3 to 4 mass transitions have been monitored, and the absolute protein abundance was assessed by using the stable isotope method and considering the protein content of the sample (data given as pmol transporter protein per mg membrane protein).

Cellular Uptake Assays. Uptake experiments were performed as described earlier (König et al., 2012). In brief, cells were seeded at an initial cell number of 7×10^5 cells per well on poly-D-lysine–coated 12-well plates. After 24 hours, cells were induced with 10 mM sodium butyrate to obtain higher protein levels. Before uptake experiments, cells were washed with prewarmed uptake buffer (142 mM NaCl, 5 mM KCl, 1 mM K_2HPO_4, 1.2 mM $MgSO_4$, 1.5 mM $CaCl_2$, 5 mM glucose, and 12.5 mM HEPES, pH 7.3). Radiolabeled substrates were dissolved in uptake buffer, and unlabeled substances were added in the respective concentrations for the uptake experiments [BSP (1 μM) and $E_2 17\beta G$ (5 μM)]. The cells were incubated with the uptake solution for 10 minute and subsequently washed three times with ice-cold uptake buffer. After the cells were lysed with 0.2% SDS, the intracellular accumulation of radioactivity was determined by liquid scintillation counting, and protein concentrations were determined by a bicinchoninic acid assay (BCA Protein Assay Kit, Thermo Fisher Scientific, Bonn Germany). The uptake of 2 μM OG was measured accordingly (without radiolabeled OG), and intracellular OG was measured using the CLARIOstar (BMG LABTECH GmbH, Ortenberg, Germany) after 10 minutes incubation by pipetting 100 μL of each cell lysate and an Oregon Green dilution series in 0.2% SDS solution into a 96-well plate. The emission was measured using the preinstalled fluorescein settings.

Colocalization Analysis. For colocalization analysis, μ-Slide 8-well glass bottom arrays (ibidi GmbH, Gräfeling, Germany) were used and coated with 200 μL poly-D-lysine. Next, 9×10^4 HEK-Kz-Ct-OATP1B3 cells per well were seeded into the μ-Slide and incubated for 24 hours at 37 °C and 5% CO_2. Afterward, either 20 μL of the CellLight lysosomes RFP, BacMam 2.0 solution per well was added or the cells were transfected with the pmScarlet-1_peroxisome_C1 plasmid by lipofection and incubated overnight. Finally, the cells were incubated with 1 μM OG solution for 1 hour, washed with PBS, and subsequently, 200 μL new culture medium was applied. OG fluorescence was measured using the preinstalled settings of the GFP channel; SPY555 was measured using the Cy3 channel of the Zen software (RRID:Addgene_85065; Carl Zeiss Microscopy GmbH, Jena, Germany). Microscopy was performed on the Zeiss Spinning Disc Axio Observer Z1 (Carl Zeiss Microscopy GmbH, Jena, Germany) at the OICE (Erlangen, Germany).

Cytotoxicity Analysis. HEK vector control (HEK-VC) and HEK-Kz-Ct-OATP1B3 cells were seeded at an initial cell number of 7×10^3 cells per well on poly-D-lysine–coated 96-well plates at a volume of 200 μL (for DLD1 cells 4×10^3 cells at 100 μL per well). After 24 hours, the kinase inhibitors (stock solutions dissolved in DMSO) were added to the respective cell culture medium. Cells were incubated for 72 hours after compound addition. For vemurafenib and regorafenib, the medium was removed, and the wells were carefully washed twice with 200 μL PBS solution. To lyse the cells, 100 μL of 0.2% SDS solution were added to each well, and the plate was shaken for 30 minutes on a 96-well plate shaker. After the lysis, 150 μL BCA solution was added, and the plate was incubated for 30 minutes at 37 °C. The absorption was measured at 560 nm using a Multiskan FC multiplate reader (Thermo Fisher Scientific Inc., Waltham, MA). The blank value was subtracted, and the absorption values were normalized with the average value of the control. Because encorafenib was interacting with the BCA assay, the CCK-8 assay was used to determine cytotoxicity. For this purpose, 10 μL CCK-8 substrate per well was added to the cells after 72 hour of compound treatment and incubated for 2 hours at 37 °C. The absorption was measured at 450 nm and normalized to the average absorption of the untreated cells. BSP was used as Ct-OATP1B3 transport inhibitor at 200 μM and was added additionally with the cytotoxic compounds, and the respective absorption values were normalized to the average absorption of cells treated with BSP only.

Quantification of Encorafenib in the Lysosomal Fraction by Mass Spectrometry. DLD1 cells were seeded at 1×10^7 cells on 10 cm plates. The cells were incubated either with 100 μM encorafenib alone or in combination with 200 μM BSP for 4 hours. Subsequently, the lysosomal fraction was enriched as described above with minor

modifications. The lysosomal pellet was first resuspended in 50 μL PBS, and 2.5 μL of this suspension was used to determine the protein amount via BCA assay. The samples were again centrifuged for 10 minutes at 17,000 *g* and 4 °C, and the PBS was removed. Each pellet was lysed in 80% MeOH/water (including the internal standard [$^2H_3$]-clopidogrel) and afterward centrifuged for 10 minutes at 25,000 *g* at 4 °C, and 200 μL of the supernatant was transferred into autosampler glass vials (Agilent, Santa Clara, CA). The solvent was evaporated using a MULTIVAP nitrogen evaporator (Organomation, Berlin, MA), and the residue was reconstituted in 100 μL solution with 90% water (containing 0.5% formic acid) and 10% MeOH (with 0.1% formic acid). The samples were measured in triplicates via an in-house method with a Q-Exactive Focus mass spectrometer coupled to a Dionex UltiMate 3000 ultrahigh-performance liquid chromatography (both Thermo Fisher Scientific, Dreieich, Germany) (Kehl et al., 2021). The area of the encorafenib peak was normalized to the peak area of the internal standard and to the protein amount of the lysosomal fraction aliquot. The data are given as percent of the average amount of encorafenib in the DLD1 cells without added BSP.

Statistical Analysis. For all transport and cytotoxicity studies, at least two independent experiments were performed on different days, each measured in triplicates or quadruplets. All data are expressed as means ± S.D. The graphs and statistical analysis were done by using GraphPad Prism (RRID:SCR_002798; Version 5.01, 2007, GraphPad Software, San Diego, CA). The statistical significance was analyzed using either one-way ANOVA with Bonferroni adjusted post hoc tests (comparison between all pairs of columns; group size = 4 if more than two cell lines were used) or a two-tailed unpaired Student's *t* test (comparison between two cell lines). For cytotoxicity experiments, *P* values were calculated for each tested kinase inhibitor concentration to demonstrate statistically different effects between HEK-VC cells and HEK-Kz-Ct-OATP1B3 cells. Due to the exploratory design of the experiment, the calculated *P* values are descriptive.

Results

Establishment of Cell Lines Recombinantly Overexpressing OATP1B3 Variants. *Ct-SLCO1B3* cDNA was cloned by an reverse transcriptase PCR–based approach using human colon cancer total RNA as template. The cDNA was inserted into the expression vector pcDNA3.1 Hygro(-), resulting in the plasmid pCt-SLCO1B3.31_Hygro. Because it has been demonstrated that a Kozak consensus sequence around the start codon of the *Ct-SLCO1B3* cDNA enhances protein expression (Imai et al., 2013), the original cDNA was mutated to contain a Kozak consensus sequence, resulting in the plasmid pKz-Ct-SLCO1B3.31_Hygro. Both plasmids were used to establish HEK293 cells recombinantly overexpressing the identical Ct-OATP1B3 protein (HEK-Ct-OATP1B3 and HEK-Kz-Ct-OATP1B3). *SLCO1B3* mRNA expression analysis was performed by quantitative reverse transcriptase PCR (Fig. 2A), showing an expression of 21.9 ± 3.04% and 56.8 ± 0.7% in HEK-Ct-OATP1B3 and HEK-Kz-Ct-OATP1B3 cells, respectively (normalized to the expression of the housekeeping gene *β-actin*). Already established HEK293 cells recombinantly overexpressing the liver-type variant of the OATP1B3 protein (HEK-Lt-OATP1B3) had a *SLCO1B3* mRNA expression of 119.7 ± 11.7% relative to the expression of *β-actin* (Seithel et al., 2007).

Immunoblot analysis using whole cell homogenates (Fig. 2B) demonstrated a fully glycosylated OATP1B3 protein in HEK-Lt-OATP1B3 cells, whereas in both cell lines expressing the Ct-OATP1B3 protein, a weak band was detectable around 75 kDa, representing the core-glycosylated form of the OATP1B3 protein (König et al., 2000). In the manuscript by König et al. (2000), the same antiserum was used. By using confocal laser scanning microscopy (Fig. 2C), we could confirm the known localization of the Lt-OATP1B3 (red staining) in the plasma membrane (sodium-potassium ATPase, green staining) of HEK-Lt-OATP1B3 cells, whereas in both cell lines expressing the Ct-OATP1B3 protein (red staining), a more intense intracellular staining could be detected in comparison with HEK-VC.

Cellular Uptake Assays. To investigate the function of the OATP1B3 proteins as uptake transporters (putatively) localized in the plasma membrane, cellular uptake assays (Taghikhani et al., 2017) were performed using the prototypic OATP1B3 substrates BSP (Fig. 3A), $E_2 17\beta G$ (Fig. 3B), and OG (Fig. 3C). All three substrates had a markedly higher uptake into HEK-Lt-OATP1B3 cells ($P < 0.001$ versus uptake into HEK-VC cells), but no differences in the uptake of HEK-Ct-OATP1B3 and HEK-Kz-Ct-OATP1B3 cells could be detected compared with the uptake into HEK-VC control cells.

Proteomics Analysis. Using a proteomics analysis, the OATP1B3 protein amount in the isolated plasma membrane fraction (Fig. 4A) and in the crude membrane fraction (Fig. 4B) of the HEK293 cells was quantified. In the isolated plasma membrane fractions, OATP1B3 protein could be detected in HEK-Lt-OATP1B3 cells but not in HEK-VC, HEK-Ct-OATP1B3, and HEK-Kz-Ct-OATP1B3 (Fig. 4A). In the crude membrane fractions of HEK-Ct-OATP1B3 and HEK-Kz-Ct-OATP1B3 cells, OATP1B3 protein could be detected but not in HEK-VC cells (Fig. 4B). Due to the high protein amount, the quantification of Lt-OATP1B3 protein was omitted in the crude membrane fraction.

Subcellular Localization of Ct-OATP1B3. For subsequent experiments, only HEK-Kz-Ct-OATP1B3 cells were used as Ct-OATP1B3 overexpressing cells because of the higher *SLCO1B3* mRNA expression. Next, the subcellular localization of the Ct-OATP1B3 protein was analyzed. In immunoblot analysis and in line with the proteomics analysis, there was no detectable protein band at 75 kDa in the isolated plasma membrane fraction of the HEK-Kz-Ct-OATP1B3 cells. However, a band could be detected in the cytosolic fraction containing intracellularly localized organelles (Fig. 4C). In contrast, a strong band at 130 kDa could be detected in HEK-Lt-OATP1B3 cells, whereas no protein was detectable in the cytosolic fraction of these cells. Next, we isolated the lysosomal fraction of HEK-Kz-Ct-OATP1B3 and HEK-VC cells and analyzed the protein abundance. Figure 4D shows an OATP1B3 protein band at 75 kDa in the enriched lysosomal fraction. Because the OATP1B3 staining using the polyclonal antiserum SKT also leads to unspecific protein binding (e.g., the protein bands in the cytosolic and lysosomal fractions at approximately 65 kDa) and the fact that no monoclonal anti–OATP1B3 antibody, which is able to detect both variants, is commercially available, a direct colocalization with lysosomal markers was not possible (data not shown). Therefore, we tried to confirm the lysosomal localization by transfecting the HEK-Kz-Ct-OATP1B3 cells either with the baculovirus-based CellLight lysosomes-RFP BacMam 2.0 system to stain the lysosomes or with the pmScarlet-1_peroxisome_C1 plasmid to stain the peroxisomes. Twenty-four hours after transfection, we incubated the cells for 1 hour with OG, a known substrate of Lt-OATP1B3 (Fig. 3C) (Izumi et al., 2016). Colocalization of the lysosomal marker with OG, resulting in a yellow color of the lysosomes, could be detected (Fig. 4E), whereas no colocalization

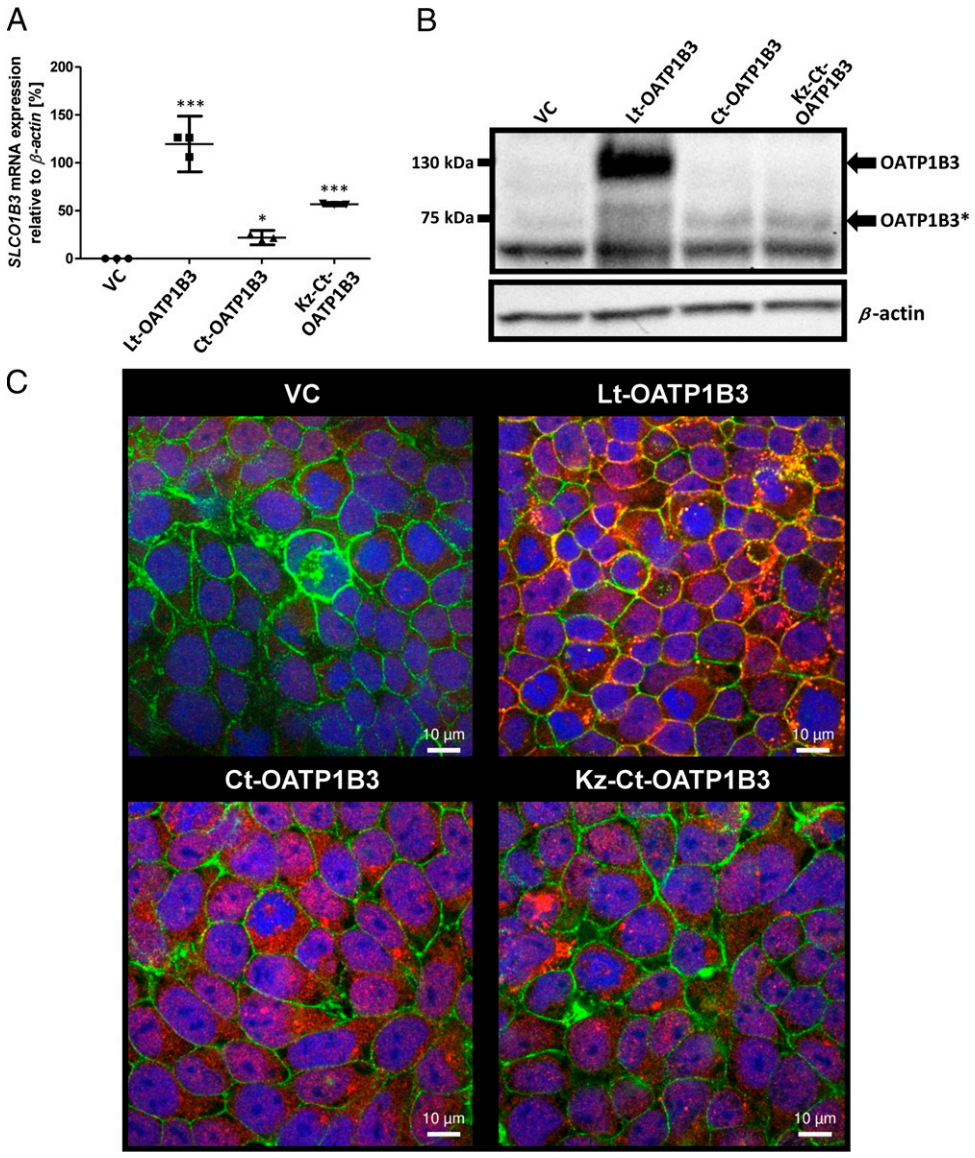

Fig. 2. Characterization of HEK293 cells stably expressing OATP1B3 variants. (A) *SLCO1B3* mRNA expression analysis. Expression is normalized to the expression of the housekeeping gene *β-actin*. Data are given as mean ± S.D. The experiment has been performed in triplicates. (B) Immunoblot analysis using whole cell homogenates. OATP1B3 was detected using the antiserum SKT; pan cadherin served as loading control. OATP1B3 represents the fully glycosylated form and OATP1B3* the core-glycosylated form. (C) Localization of OATP1B3 variants (red) analyzed by confocal laser scanning microscopy. The sodium-potassium ATPase (green) was used as membrane marker; the nuclei are shown in blue. Yellow color results from the colocalization of the membrane marker with the OATP1B3 protein. In both cell lines expressing the Ct-OATP1B3 protein, a more intense intracellular staining compared with the staining in the control cells could be detected. Scale bar, 10 μm. ***$P < 0.001$ Lt-OATP1B3, Kz-Ct-OATP1B3 versus VC; *$P < 0.05$ Ct-OATP1B3 versus VC. VC, HEK293 cells transfected with the empty vector; Lt-OATP1B3, HEK293 cells recombinantly overexpressing the liver-type variant of OATP1B3; Ct-OATP1B3, HEK293 cells transfected with the cancer-type variant of OATP1B3; Kz-Ct-OATP1B3, HEK293 cells recombinantly overexpressing the cancer-type variant of OATP1B3 with a Kozak sequence around the start codon.

could be detected between OG-stained vesicles and the stained peroxisomes (Fig. 4F; Supplemental Fig. 1), indicating lysosomal localization of the Ct-OATP1B3 protein.

Cytotoxicity of Kinase Inhibitors. To investigate the function of Ct-OATP1B3 localized in lysosomes, we used the BRAF inhibitor vemurafenib, substrate and inhibitor of Lt-OATP1B3 (Zimmerman et al., 2013; Kayesh et al., 2021) and the BRAF inhibitor encorafenib, approved for the treatment of metastatic colorectal cancer in combination with cetuximab. In addition, we used the vascular endothelial growth factor receptor inhibitor regorafenib (also approved for the treatment of metastatic colorectal cancer), which is not a substrate or inhibitor of Lt-OATP1B3 (https://www.accessdata.fda.gov/drugsatfda_docs/nda/2013/204369Orig1s000ClinPharmR.pdf; Ohya et al., 2015). HEK-Kz-Ct-OATP1B3 and HEK-VC cells were incubated with the respective kinase inhibitor at different concentrations, and the number of surviving cells was determined (Fig. 5).

Expression of the Ct-OATP1B3 protein led to better survival when cells were incubated with encorafenib (Fig. 5A). A slight effect of Ct-OATP1B3 expression was detected for vemurafenib (Fig. 5B; $P = 0.051$ at 100 μM), whereas the survival curves of both cell lines were nearly identical when treated with regorafenib (Fig. 5C). This indicates that Ct-OATP1B3 expression may confer resistance against kinase inhibitors and that this resistance is substrate dependent.

Ct-OATP1B3 in the Colorectal Cancer Cell Lines DLD1 and T84. Additionally, the *Ct-SLCO1B3* mRNA and Ct-OATP1B3 protein analysis were performed in the two colorectal carcinoma cell lines T84 and DLD1. Both cell lines endogenously express *Ct-SLCO1B3* mRNA (Fig. 6A). Furthermore, Ct-OATP1B3 protein expression could be verified in immunoblot (Fig. 6B) and proteomics analysis (Fig. 6C). The protein band of Ct-OATP1B3 could also be detected in the enriched lysosomal fractions of both cell lines (Fig. 6D).

In DLD1 cells, we inhibited the potential Ct-OATP1B3–mediated substrate transport into lysosomes in the cytotoxicity assays by adding the OATP1B3 substrate BSP (200 μM). When added in combination with the same kinase inhibitors

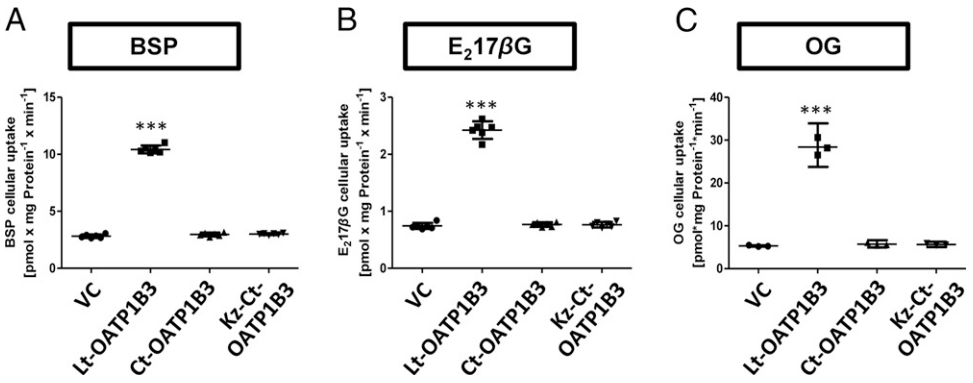

Fig. 3. Cellular uptake assays using prototypic OATP1B3 substrates. Intracellular accumulation of (A) 1 μM bromosulphophthalein (BSP), (B) 5 μM estradiol-17β-glucuronide ($E_2$17βG), and (C) 2 μM Oregon Green 488 (OG) into the stable transfectants. Data are given as mean ± S.D. The experiments have been performed twice in triplicates. ***$P < 0.001$ Lt-OATP1B3 versus VC, Ct-OATP1B3, and Kz-Ct-OATP1B3.

used in HEK293 cell experiments, BSP led to an increase in the cytotoxic effects of encorafenib (Fig. 7A) and vemurafenib (Fig. 7B). Interestingly, for regorafenib, the addition of BSP led to a markedly higher survival in the DLD1 cells ($P <$ 0.001 at 100 μM; Fig. 7C). To verify whether the increase in the cytotoxicity of encorafenib is due to an inhibition of the lysosomal sequestration, we incubated DLD1 cells with encorafenib (100 μM) alone or in combination with BSP for 4 hours, isolated the enriched lysosomal fraction, and quantified the amount of this kinase inhibitor. Due to transport inhibition, the addition of BSP led to a reduction of encorafenib in the enriched lysosomal fraction ($P < 0.001$; Fig. 7D).

Discussion

The aim of this study was to gain insights into the expression, localization, and function of the Ct-OATP1B3 protein and to clarify previously published inconsistent results regarding these issues. Therefore, we established stably transfected HEK293 cells recombinantly overexpressing this transport protein and investigated protein amount and localization, Ct-OATP1B3–mediated transport, and a possible function of Ct-OATP1B3 expression in transfected HEK293 cells and colorectal cancer cells. Our results demonstrate that Ct-OATP1B3 protein is localized in lysosomes mediating the transport of substances into these intracellular vesicles. Furthermore, expression of Ct-OATP1B3 protein led to a better survival of cells when treated with the kinase inhibitor encorafenib, used for the treatment of metastatic colorectal cancer.

Before Nagai et al. (2012) characterized the *Ct-SLCO1B3*-mRNA as a splice variant of the *SLCO1B3* gene expressed in colorectal cancer tissue, several authors described OATP1B3 overexpression in different cancerous tissues without discriminating between the Lt- and Ct-OATP1B3 variant (Abe et al., 2001; Lee et al., 2008; Lockhart et al., 2008). Hence, these older studies may need re-evaluation on this background, and further studies should discriminate between both variants (Alam et al., 2018; Sun et al., 2020). For example, Alam et al. (2018) identified mRNA expression of both variants in breast cancer samples, whereas Thakkar et al. (2013) detected only *Ct-SLCO1B3*-mRNA in CRC samples. This discrimination of both variants could also help to explain the described varying *SLCO1B3*-correlated outcomes in breast cancer (Muto et al., 2007; Tang et al., 2021) and CRC (Teft et al., 2015; Zhi et al., 2021). Furthermore, the published results obtained with CRC cells transfected with the cDNA encoding the Lt-OATP1B3 protein (Lee et al., 2008; Niedermeyer et al., 2014) are difficult to interpret because the localization of Ct-OATP1B3 is altered due to the truncated aminoterminal end (Chun et al., 2017). This altered localization of the Ct-OATP1B3 protein could be verified with the present work since no Ct-OATP1B3 protein could be detected in the isolated plasma membrane fraction (Fig. 4A), but low amounts were detectable in the crude membrane fraction (Fig. 4B). In addition, this aminoterminal truncation seems to affect the glycosylation of the Ct-OATP1B3 protein (Fig. 2B), resulting in a band with a molecular mass of approximately 75 kDa (König et al., 2000; Ho et al., 2006). Similar results were obtained by analyzing Ct-OATP1B3 expression in the colorectal carcinoma cell line HCT-116 and the pancreatic cancer cell line Panc-1 (Thakkar et al., 2013) and by analyzing the N-linked glycosylation of Lt-OATP1B3 in nonalcoholic fatty liver disease (Clarke et al., 2017). Additionally, the results of the cellular uptake experiments (Fig. 3), which showed no difference between the Ct-OATP1B3 transfectants and HEK-VC, are in line with the intracellular localization of Ct-OATP1B3 and with the previously described lack of transport function (Thakkar et al., 2013).

Because unspecific antiserum binding of the polyclonal antiserum SKT and the low protein translation efficiency, especially in stably transfected HEK293 cells, limit the methods of protein detection, colocalization studies were used to identify the vesicles containing the Ct-OATP1B3 protein. Using the fluorescent dye and known OATP1B3 substrate OG, we analyzed the potential transport function of Ct-OATP1B3 protein located in intracellular vesicles (Fig. 4, E and F) and identified these vesicles as lysosomes by cotransfection with the lysosomal marker BacMam Lysosomes-RFP (Fig. 4E). Interestingly, this lysosomal localization may be of special interest for the possible function of Ct-OATP1B3 protein expression in cancer cells. Lysosomal sequestration has been described for various drugs used in antitumor therapy, especially some kinase inhibitors (e.g., nintendanib, sunitinib) (Krchniakova et al., 2020). This sequestration leads to a reduced cytoplasmic concentration of these drugs and consequently results in a higher cytotoxic resistance (Englinger et al., 2017). So far, this kind of transport has been attributed to the function of ABC transporters [e.g., ABCA3, P-glycoprotein] localized in lysosomal membranes (Chapuy et al., 2009; Yamagishi et al., 2013). Our cytotoxicity experiments (Fig. 5) demonstrated that overexpression of the SLC transporter Ct-OATP1B3 led to a better survival of cells when incubated with selected kinase inhibitors, suggesting that also SLC transporters located in intracellular vesicles may be important for this resistance mechanism.

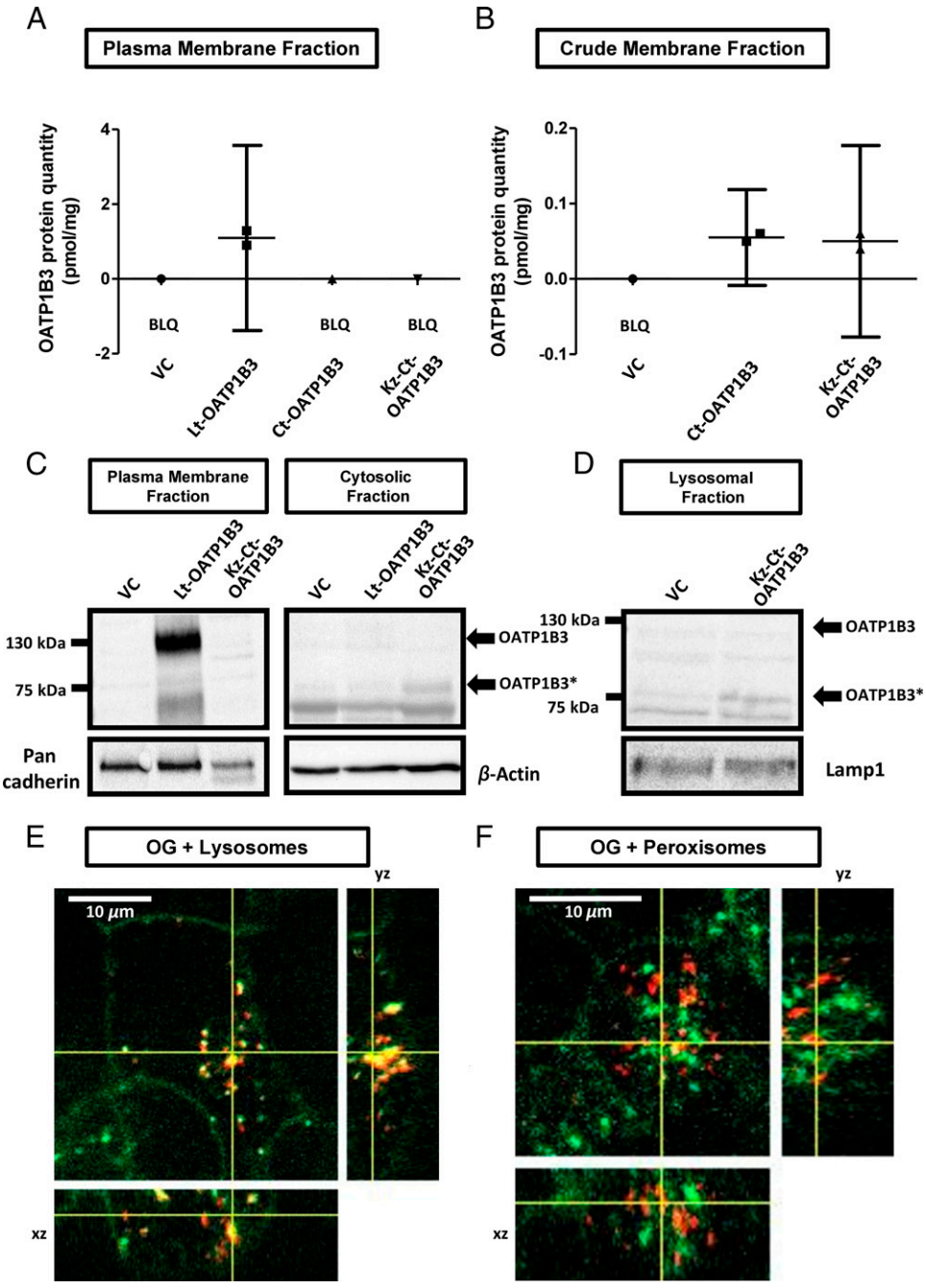

Fig. 4. Proteomics-based expression analysis and subcellular localization of Ct-OATP1B3. Amount of OATP1B3 protein in (A) the isolated plasma membrane fraction and in (B) preparations of crude membrane fraction of the stable transfectants determined by mass spectrometry. Due to the high protein amount, the quantification of Lt-OATP1B3 protein was omitted in the crude membrane fraction. Experiments were performed once with $n = 2$. (C) Immunoblot analysis of the plasma membrane fraction and the cytosolic fraction of the stably transfected HEK293 cells. β-Actin served as loading control. OATP1B3 represents the fully glycosylated form and OATP1B3* the core-glycosylated form. (D) Analysis of the enriched lysosomal fraction. The lysosomal marker Lamp1 served as loading control. (E and F) HEK-Kz-Ct-OATP1B3 cells were seeded in a μ-slide 8-well glass bottom array, and 24 hours after seeding, cells were transfected with (E) the CellLight lysosomes-RFP, BacMam 2.0 system or with (F) the pmScarlet-1_peroxisome_C1 plasmid. One hour prior to the experiments, the cells were preincubated with 1 μM OG, a known substrate of OATP1B3. The cells were analyzed via confocal laser scanning microscopy. Scale bar, 10 μm. BLQ, amount below limit of quantification.

Zimmermann et al. (2013) could demonstrate a considerably higher uptake of vemurafenib into stable-transfected HEK293 cells overexpressing Lt-OATP1B3 compared with the HEK293 control cell line. The other BRAF inhibitor encorafenib is not described as substrate for the Lt-OATP1B3 protein so far and did not show an enhanced uptake into HEK-Lt-OATP1B3 cells compared with the control cell line in our experiments (Supplemental Fig. 2), but both BRAF inhibitors are mentioned as inhibitors of Lt-OATP1B3–mediated transport by the Food and Drug Administration (https://www.accessdata.fda.gov/drugsatfda_docs/nda/2011/202429Orig1s000ClinPharmR.pdf; https://www.accessdata.fda.gov/drugsatfda_docs/nda/2018/210496Orig1s000MultidisciplineR.pdf). Notably, the tested concentrations of vemurafenib in this study were in the concentration range of its reported plasma trough concentrations in humans (Verheijen et al., 2017; Mueller-Schoell et al., 2021), underlining a potential in vivo relevance of Ct-OATP1B3. This was recently reported for OATP1B3 protein without discriminating between the Lt- and Ct-OATP1B3 protein (Kayesh et al., 2021). It should be noted that the cytoprotective effect of Ct-OATP1B3 expression is not a general effect for all kinase inhibitors as we could show with regorafenib, which is neither a substrate nor inhibitor of Lt-OATP1B3 (Fig. 5C) (https://www.accessdata.fda.gov/drugsatfda_docs/nda/2013/204369Orig1s000ClinPharmR.pdf; Ohya et al., 2015). Interestingly, the protective effect of Ct-OATP1B3 expression was diminished by the coapplication of the Lt-OATP1B3 substrate BSP together with encorafenib (Fig. 7A) or vemurafenib

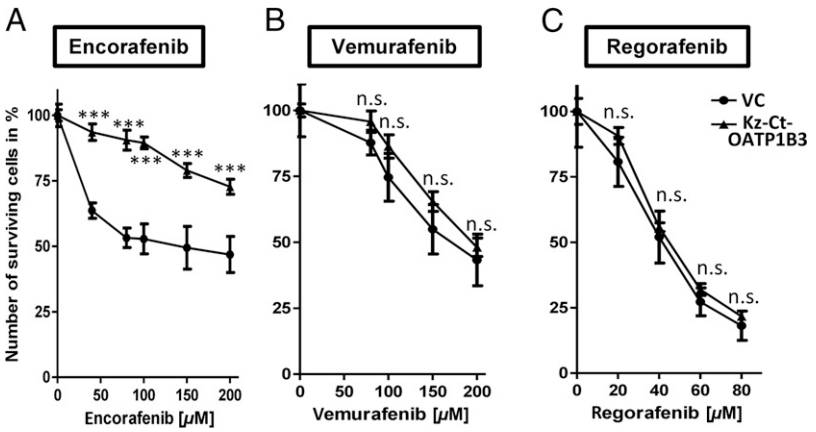

Fig. 5. Cytotoxicity of kinase inhibitors analyzed in stably transfected HEK293 cells. Cytotoxicity of (A) encorafenib (two experiments measured in quadruplets), (B) vemurafenib (two experiments measured in quadruplets), and (C) regorafenib (three experiments measured in quadruplets) determined by BCA assay (vemurafenib, regorafenib) or CCK-8 assay (encorafenib) after 72 hours of drug exposure. Data are presented as mean ± S.D. ***$P < 0.001$ Kz-Ct-OATP1B3 versus VC. n.s., not significant.

(Fig. 7B) in DLD1 cells endogenously expressing Ct-OATP1B3. In this experimental setup, the Ct-OATP1B3–mediated transport of both kinase inhibitors into lysosomes seems to be inhibited, resulting in an increased cytotoxicity of treated DLD1 cells. In line with these results, the amount of encorafenib in the enriched lysosomal fraction was reduced (Fig. 7D). It can be speculated that Ct-OATP1B3–mediated resistance could contribute to insufficient clinical effects of monotherapy of BRAF inhibitors in colorectal cancer (Prahallad et al., 2012; Mao et al., 2013; Yaeger et al., 2017).

Taken together, we could demonstrate that Ct-OATP1B3 protein, a splice variant of the liver-type uptake transporter Lt-OATP1B3, is localized in lysosomes and is capable of transporting Ct-OATP1B3 substrates into these vesicles. Furthermore, as shown for encorafenib, the substrate spectrum between the Ct-OATP1B3 and the Lt-OATP1B3 protein seems to be different, and further studies are necessary to gain insights into the substrate spectrum of the Ct-OATP1B3 protein. When treated with kinase inhibitors, the expression of Ct-OATP1B3 protein led to a better survival of cells by

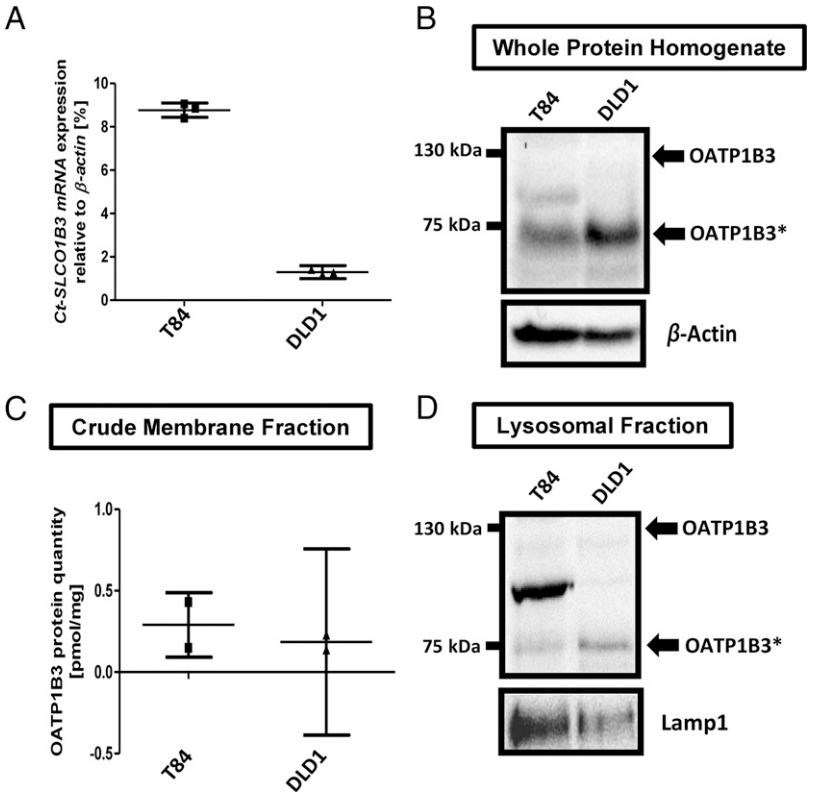

Fig. 6. *Ct-SLCO1B3* mRNA and Ct-OATP1B3 protein expression in the colorectal carcinoma cell lines T84 and DLD1. (A) Quantification of the *Ct-SLCO1B3* mRNA expression in T84 and DLD1 cells. Expression is normalized to the mRNA expression of the housekeeping gene *β-actin* and measured once in triplicates. (B) Ct-OATP1B3 protein expression in T84 and DLD1 cells using whole cell homogenate in the immunoblot analysis and (C) the crude membrane fraction in the proteomics analysis ($n = 2$). (D) Ct-OATP1B3 protein expression in the enriched lysosomal fraction of the CRC cells. Lamp1 served as lysosomal marker.

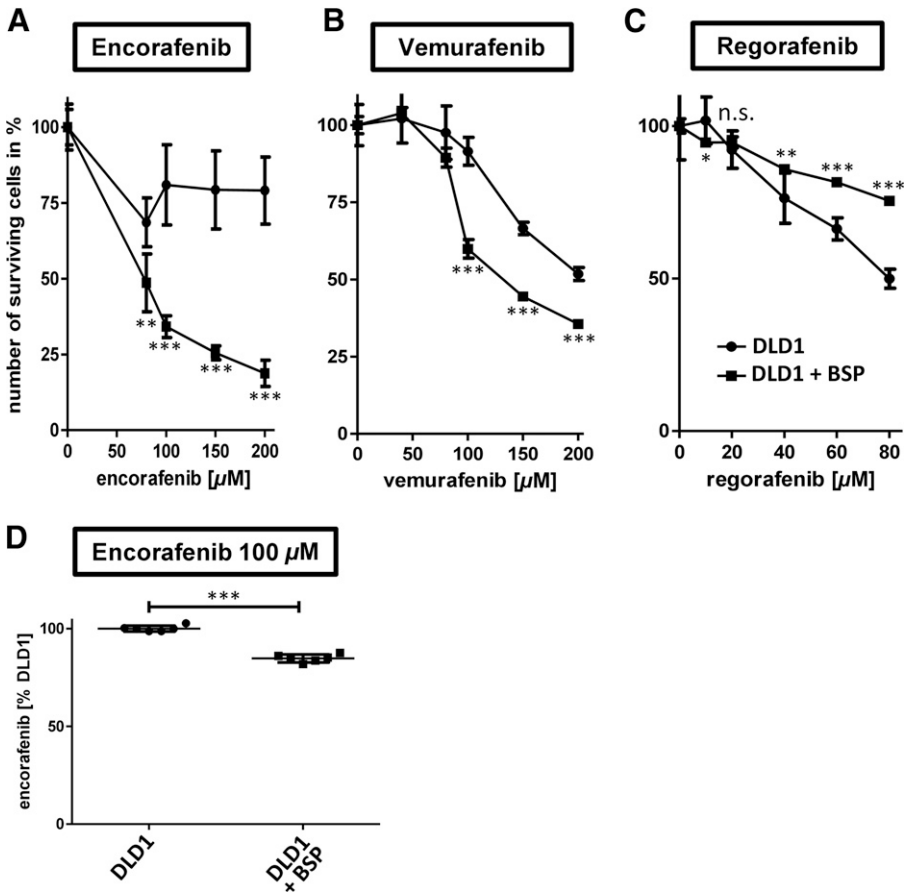

Fig. 7. Effect of Ct-OATP1B3–mediated transport inhibition in DLD1 cells. Cytotoxicity of (A) encorafenib, (B) vemurafenib, and (C) regorafenib in DLD1 cells with and without coincubation of the cells with BSP (200 μM), measured after 72 hour of compound treatment. Experiments were performed twice measured in quadruplets. (D) Quantification of encorafenib in the isolated lysosomal fraction after 4-hour drug exposure with and without added BSP (two experiments measured in triplicates). ***$P < 0.001$ DLD1 versus DLD1 + BSP; **$P < 0.01$ DLD1 versus DLD1 + BSP; *$P < 0.05$ DLD1 versus DLD1 + BSP. n.s., not significant.

transporting these cytotoxic compounds into lysosomes, thereby reducing their cytoplasmic concentration. This is a new kind of a Ct-OATP1B3–mediated resistance mechanism against antitumor drugs and in line with the association of a higher *Ct-SLCO1B3* expression and a reduced progression-free survival or overall survival of colorectal cancer patients (Teft et al., 2015; Zhi et al., 2021). Its importance for the therapy of other tumor entities expressing Ct-OATP1B3 or for other antitumor drugs that are substrates of this transport protein needs to be elucidated in the future. Furthermore, these results suggest that the expression of Ct-OATP1B3 protein in tumor tissues may serve as an important biomarker for patients treated with antitumor drugs.

Acknowledgments

We thank Olga Stelmakh and Claudia Hoffmann for their technical assistance. Microscopy analysis was performed with the support of the OICE and Dr. Philipp Tripal, Dr. Benjamin Schmidt, and Dr. Zoltán Winter. DLD1 and T84 cells were kindly provided by Dr. Britzen-Laurent and Dr. Naschberger (Erlangen, Germany).

Authorship Contributions

Participated in research design: Haberkorn, Oswald, Gessner, Taudte, Zunke, Fromm, König.

Conducted experiments: Haberkorn, Oswald, Kehl, Dobert.

Contributed new reagents or analytic tools: Oswald, Gessner, Taudte, Dobert, Zunke.

Performed data analysis: Haberkorn, Oswald, König.

Wrote or contributed to the writing of the manuscript: Haberkorn, Oswald, Kehl, Gessner, Taudte, Dobert, Zunke, Fromm, König.

References

Abe T, Unno M, Onogawa T, Tokui T, Kondo TN, Nakagomi R, Adachi H, Fujiwara K, Okabe M, Suzuki T, et al. (2001) LST-2, a human liver-specific organic anion transporter, determines methotrexate sensitivity in gastrointestinal cancers. *Gastroenterology* **120**:1689–1699.

Al-Abdulla R, Perez-Silva L, Abete L, Romero MR, Briz O, and Marin JJG (2019) Unraveling 'The Cancer Genome Atlas' information on the role of SLC transporters in anticancer drug uptake. *Expert Rev Clin Pharmacol* **12**:329–341.

Alam K, Farasyn T, Ding K, and Yue W (2018) Characterization of liver- and cancer-type-organic anion transporting polypeptide (OATP) 1B3 messenger RNA expression in normal and cancerous human tissues. *Drug Metab Lett* **12**:24–32.

Chapuy B, Panse M, Radunski U, Koch R, Wenzel D, Inagaki N, Haase D, Truemper L, and Wulf GG (2009) ABC transporter A3 facilitates lysosomal sequestration of imatinib and modulates susceptibility of chronic myeloid leukemia cell lines to this drug. *Haematologica* **94**:1528–1536.

Chun SE, Thakkar N, Oh Y, Park JE, Han S, Ryoo G, Hahn H, Maeng SH, Lim YR, Han BW, et al. (2017) The N-terminal region of organic anion transporting polypeptide 1B3 (OATP1B3) plays an essential role in regulating its plasma membrane trafficking. *Biochem Pharmacol* **131**:98–105.

Clarke JD, Novak P, Lake AD, Hardwick RN, and Cherrington NJ (2017) Impaired N-linked glycosylation of uptake and efflux transporters in human non-alcoholic fatty liver disease. *Liver Int* **37**:1074–1081.

Drozdzik M, Busch D, Lapczuk J, Müller J, Ostrowski M, Kurzawski M, and Oswald S (2019) Protein abundance of clinically relevant drug transporters in the human liver and intestine: a comparative analysis in paired tissue specimens. *Clin Pharmacol Ther* **105**:1204–1212.

Englinger B, Kallus S, Senkiv J, Heilos D, Gabler L, van Schoonhoven S, Terenzi A, Moser P, Pirker C, Timelthaler G, et al. (2017) Intrinsic fluorescence of the clinically

approved multikinase inhibitor nintedanib reveals lysosomal sequestration as resistance mechanism in FGFR-driven lung cancer. *J Exp Clin Cancer Res* **36**:122.
Fahrmayr C, Fromm MF, and König J (2010) Hepatic OATP and OCT uptake transporters: their role for drug-drug interactions and pharmacogenetic aspects. *Drug Metab Rev* **42**:380–401.
Gröer C, Brück S, Lai Y, Paulick A, Busemann A, Heidecke CD, Siegmund W, and Oswald S (2013) LC-MS/MS-based quantification of clinically relevant intestinal uptake and efflux transporter proteins. *J Pharm Biomed Anal* **85**:253–261.
Hamada A, Sissung T, Price DK, Danesi R, Chau CH, Sharifi N, Venzon D, Maeda K, Nagao K, Sparreboom A, et al. (2008) Effect of *SLCO1B3* haplotype on testosterone transport and clinical outcome in caucasian patients with androgen-independent prostatic cancer. *Clin Cancer Res* **14**:3312–3318.
Hays A, Apte U, and Hagenbuch B (2013) Organic anion transporting polypeptides expressed in pancreatic cancer may serve as potential diagnostic markers and therapeutic targets for early stage adenocarcinomas. *Pharm Res* **30**:2260–2269.
Ho RH, Tirona RG, Leake BF, Glaeser H, Lee W, Lemke CJ, Wang Y, and Kim RB (2006) Drug and bile acid transporters in rosuvastatin hepatic uptake: function, expression, and pharmacogenetics. *Gastroenterology* **130**:1793–1806.
Huang KM, Uddin ME, DiGiacomo D, Lustberg MB, Hu S, and Sparreboom A (2020) Role of *SLC* transporters in toxicity induced by anticancer drugs. *Expert Opin Drug Metab Toxicol* **16**:493–506.
Imai S, Kikuchi R, Tsuruya Y, Naoi S, Nishida S, Kusuhara H, and Sugiyama Y (2013) Epigenetic regulation of organic anion transporting polypeptide 1B3 in cancer cell lines. *Pharm Res* **30**:2880–2890.
Izumi S, Nozaki Y, Komori T, Takenaka O, Maeda K, Kusuhara H, and Sugiyama Y (2016) Investigation of fluorescein derivatives as substrates of organic anion transporting polypeptide (OATP) 1B1 to develop sensitive fluorescence-based OATP1B1 inhibition assays. *Mol Pharm* **13**:438–448.
Kayesh R, Farasyn T, Crowe A, Liu Q, Pahwa S, Alam K, Neuhoff S, Hatley O, Ding K, and Yue W (2021) Assessing OATP1B1- and OATP1B3-mediated drug-drug interaction potential of vemurafenib using R-value and physiologically-based pharmacokinetic models. *J Pharm Sci* **110**:314–324.
Kehl N, Schlichtig K, Dürr P, Bellut L, Dörje F, Fietkau R, Pavel M, Mackensen A, Wullich B, Maas R, et al. (2021) An easily expandable multi-drug LC-MS assay for the simultaneous quantification of 57 oral antitumor drugs in human plasma. *Cancers (Basel)* **13**:6329
König J, Cui Y, Nies AT, and Keppler D (2000) Localization and genomic organization of a new hepatocellular organic anion transporting polypeptide. *J Biol Chem* **275**: 23161–23168.
König J, Klatt S, Dilger K, and Fromm MF (2012) Characterization of ursodeoxycholic and norursodeoxycholic acid as substrates of the hepatic uptake transporters OATP1B1, OATP1B3, OATP2B1 and NTCP. *Basic Clin Pharmacol Toxicol* **111**:81–86.
Kounnis V, Ioachim E, Svoboda M, Tzakos A, Sainis I, Thalhammer T, Steiner G, and Briasoulis E (2011) Expression of organic anion-transporting polypeptides 1B3, 1B1, and 1A2 in human pancreatic cancer reveals a new class of potential therapeutic targets. *OncoTargets Ther* **4**:27–32.
Krchniakova M, Skoda J, Neradil J, Chlapek P, and Veselska R (2020) Repurposing tyrosine kinase inhibitors to overcome multidrug resistance in cancer: a focus on transporters and lysosomal sequestration. *Int J Mol Sci* **21**:3157.
Lee W, Belkhiri A, Lockhart AC, Merchant N, Glaeser H, Harris EI, Washington MK, Brunt EM, Zaika A, Kim RB, et al. (2008) Overexpression of OATP1B3 confers apoptotic resistance in colon cancer. *Cancer Res* **68**:10315–10323.
Locher KP (2016) Mechanistic diversity in ATP-binding cassette (ABC) transporters. *Nat Struct Mol Biol* **23**:487–493.
Lockhart AC, Harris E, Lafleur BJ, Merchant NB, Washington MK, Resnick MB, Yeatman TJ, and Lee W (2008) Organic anion transporting polypeptide 1B3 (OATP1B3) is overexpressed in colorectal tumors and is a predictor of clinical outcome. *Clin Exp Gastroenterol* **1**:1–7.
Mao M, Tian F, Mariadason JM, Tsao CC, Lemos Jr R, Dayyani F, Gopal YN, Jiang ZQ, Wistuba II, Tang XM, et al. (2013) Resistance to BRAF inhibition in BRAF-mutant colon cancer can be overcome with PI3K inhibition or demethylating agents. *Clin Cancer Res* **19**:657–667.
Mazzulli JR, Xu YH, Sun Y, Knight AL, McLean PJ, Caldwell GA, Sidransky E, Grabowski GA, and Krainc D (2011) Gaucher disease glucocerebrosidase and α-synuclein form a bidirectional pathogenic loop in synucleinopathies. *Cell* **146**:37–52.
Moitra K and Dean M (2011) Evolution of ABC transporters by gene duplication and their role in human disease. *Biol Chem* **392**:29–37.
Mueller-Schoell A, Groenland SL, Scherf-Clavel O, van Dyk M, Huisinga W, Michelet R, Jaehde U, Steeghs N, Huitema ADR, and Kloft C (2021) Therapeutic drug monitoring of oral targeted antineoplastic drugs. *Eur J Clin Pharmacol* **77**:441–464.
Muto M, Onogawa T, Suzuki T, Ishida T, Rikiyama T, Katayose Y, Ohuchi N, Sasano H, Abe T, and Unno M (2007) Human liver-specific organic anion transporter-2 is a potent prognostic factor for human breast carcinoma. *Cancer Sci* **98**:1570–1576.
Nagai M, Furihata T, Matsumoto S, Ishii S, Motohashi S, Yoshino I, Ugajin M, Miyajima A, Matsumoto S, and Chiba K (2012) Identification of a new organic anion transporting polypeptide 1B3 mRNA isoform primarily expressed in human cancerous tissues and cells. *Biochem Biophys Res Commun* **418**:818–823.
Neul C, Schaeffeler E, Sparreboom A, Laufer S, Schwab M, and Nies AT (2016) Impact of membrane drug transporters on resistance to small-molecule tyrosine kinase inhibitors. *Trends Pharmacol Sci* **37**:904–932.
Niedermeyer TH, Daily A, Swiatecka-Hagenbruch M, and Moscow JA (2014) Selectivity and potency of microcystin congeners against OATP1B1 and OATP1B3 expressing cancer cells. *PLoS One* **9**:e91476.
Ogane N, Yasuda M, Kameda Y, Yokose T, Kato H, Itoh A, Nishino S, Hashimoto Y, and Kamoshida S (2013) Prognostic value of organic anion transporting polypeptide 1B3 and copper transporter 1 expression in endometrial cancer patients treated with paclitaxel and carboplatin. *Biomed Res* **34**:143–151.
Ohya H, Shibayama Y, Ogura J, Narumi K, Kobayashi M, and Iseki K (2015) Regorafenib is transported by the organic anion transporter 1B1 and the multidrug resistance protein 2. *Biol Pharm Bull* **38**:582–586.
Pizzagalli MD, Bensimon A, and Superti-Furga G (2021) A guide to plasma membrane solute carrier proteins. *FEBS J* **288**:2784–2835.
Prahallad A, Sun C, Huang S, Di Nicolantonio F, Salazar R, Zecchin D, Beijersbergen RL, Bardelli A, and Bernards R (2012) Unresponsiveness of colon cancer to BRAF(V600E) inhibition through feedback activation of EGFR. *Nature* **483**:100–103.
Pressler H, Sissung TM, Venzon D, Price DK, and Figg WD (2011) Expression of OATP family members in hormone-related cancers: potential markers of progression. *PLoS One* **6**:e20372 10.1371/journal.pone.0020372.
Robey RW, Pluchino KM, Hall MD, Fojo AT, Bates SE, and Gottesman MM (2018) Revisiting the role of ABC transporters in multidrug-resistant cancer. *Nat Rev Cancer* **18**:452–464.
Roth M, Obaidat A, and Hagenbuch B (2012) OATPs, OATs and OCTs: the organic anion and cation transporters of the *SLCO* and *SLC22A* gene superfamilies. *Br J Pharmacol* **165**:1260–1287.
Seithel A, Eberl S, Singer K, Auge D, Heinkele G, Wolf NB, Dörje F, Fromm MF, and König J (2007) The influence of macrolide antibiotics on the uptake of organic anions and drugs mediated by OATP1B1 and OATP1B3. *Drug Metab Dispos* **35**:779–786.
Seithel A, Glaeser H, Fromm MF, and König J (2008) The functional consequences of genetic variations in transporter genes encoding human organic anion-transporting polypeptide family members. *Expert Opin Drug Metab Toxicol* **4**:51–64.
Sun R, Ying Y, Tang Z, Liu T, Shi F, Li H, Guo T, Huang S, and Lai R (2020) The emerging role of the SLCO1B3 protein in cancer resistance. *Protein Pept Lett* **27**:17–29.
Sun Y, Furihata T, Ishii S, Nagai M, Harada M, Shimozato O, Kamijo T, Motohashi S, Yoshino I, Kamiichi A, et al. (2014) Unique expression features of cancer-type organic anion transporting polypeptide 1B3 mRNA expression in human colon and lung cancers. *Clin Transl Med* **3**:37 10.1186/s40169-014-0037-y.
Taghikhani E, Fromm MF, and König J (2017) Assays for analyzing the role of transport proteins in the uptake and the vectorial transport of substances affecting cell viability, in *Cell Viability Assays Methods in Molecular Biology* (Gilbert D and Friedrich O, eds) pp 123–135, Humana Press, New York.
Taghikhani E, Maas R, Fromm MF, and König J (2019) The renal transport protein OATP4C1 mediates uptake of the uremic toxin asymmetric dimethylarginine (ADMA) and efflux of cardioprotective L-homoarginine. *PLoS One* **14**: e0213747.
Taghikhani E, Maas R, Taudte RV, Gessner A, Fromm MF, and König J (2020) Vectorial transport of the arginine derivatives asymmetric dimethylarginine (ADMA) and L-homoarginine by OATP4C1 and P-glycoprotein studied in double-transfected MDCK cells. *Amino Acids* **52**:975–985.
Tang T, Wang G, Liu S, Zhang Z, Liu C, Li F, Liu X, Meng L, Yang H, Li C, et al. (2021) Highly expressed SLCO1B3 inhibits the occurrence and development of breast cancer and can be used as a clinical indicator of prognosis. *Sci Rep* **11**:631 .
Teft WA, Welch S, Lenehan J, Parfitt J, Choi YH, Winquist E, and Kim RB (2015) OATP1B1 and tumour OATP1B3 modulate exposure, toxicity, and survival after irinotecan-based chemotherapy. *Br J Cancer* **112**:857–865.
Thakkar N, Kim K, Jang ER, Han S, Kim K, Kim D, Merchant N, Lockhart AC, and Lee W (2013) A cancer-specific variant of the *SLCO1B3* gene encodes a novel human organic anion transporting polypeptide 1B3 (OATP1B3) localized mainly in the cytoplasm of colon and pancreatic cancer cells. *Mol Pharm* **10**:406–416.
Verheijen RB, Yu H, Schellens JHM, Beijnen JH, Steeghs N, and Huitema ADR (2017) Practical recommendations for therapeutic drug monitoring of kinase inhibitors in oncology. *Clin Pharmacol Ther* **102**:765–776.
Yaeger R, Yao Z, Hyman DM, Hechtman JF, Vakiani E, Zhao H, Su W, Wang L, Joelson A, Cercek A, et al. (2017) Mechanisms of acquired resistance to BRAF V600E inhibition in colon cancers converge on RAF dimerization and are sensitive to its inhibition. *Cancer Res* **77**:6513–6523.
Yamagishi T, Sahni S, Sharp DM, Arvind A, Jansson PJ, and Richardson DR (2013) P-glycoprotein mediates drug resistance via a novel mechanism involving lysosomal sequestration. *J Biol Chem* **288**:31761–31771.
Zhang Y and Wang J (2020) Targeting uptake transporters for cancer imaging and treatment. *Acta Pharm Sin B* **10**:79–90.
Zhi L, Zhao L, Zhang X, Liu W, Gao B, Wang F, Wang X, and Wang G (2021) *SLCO1B3* promotes colorectal cancer tumorigenesis and metastasis through STAT3. *Aging (Albany NY)* **13**:22164–22175.
Zimmerman EI, Hu S, Roberts JL, Gibson AA, Orwick SJ, Li L, Sparreboom A, and Baker SD (2013) Contribution of OATP1B1 and OATP1B3 to the disposition of sorafenib and sorafenib-glucuronide. *Clin Cancer Res* **19**:1458–1466.

Address correspondence to: Dr. Jörg König, Institute of Experimental and Clinical Pharmacology and Toxicology, Clinical Pharmacology and Clinical Toxicology, Friedrich-Alexander-Universität Erlangen-Nürnberg, Fahrstrasse 17, 91054 Erlangen, Germany. E-mail: joerg.koenig@fau.de

Supplemental Data: Cancer-type organic anion transporting polypeptide 1B3 (Ct-OATP1B3) is localized in lysosomes and mediates resistance against kinase inhibitors

Authors: Bastian Haberkorn , Stefan Oswald , Niklas Kehl, Arne Gessner, R. Verena Taudte, Jan Philipp Dobert , Friederike Zunke, Martin F. Fromm and Jörg König

Journal Name: Molecular Pharmacology

Manuscript: MOLPHARM-AR-2022-000539

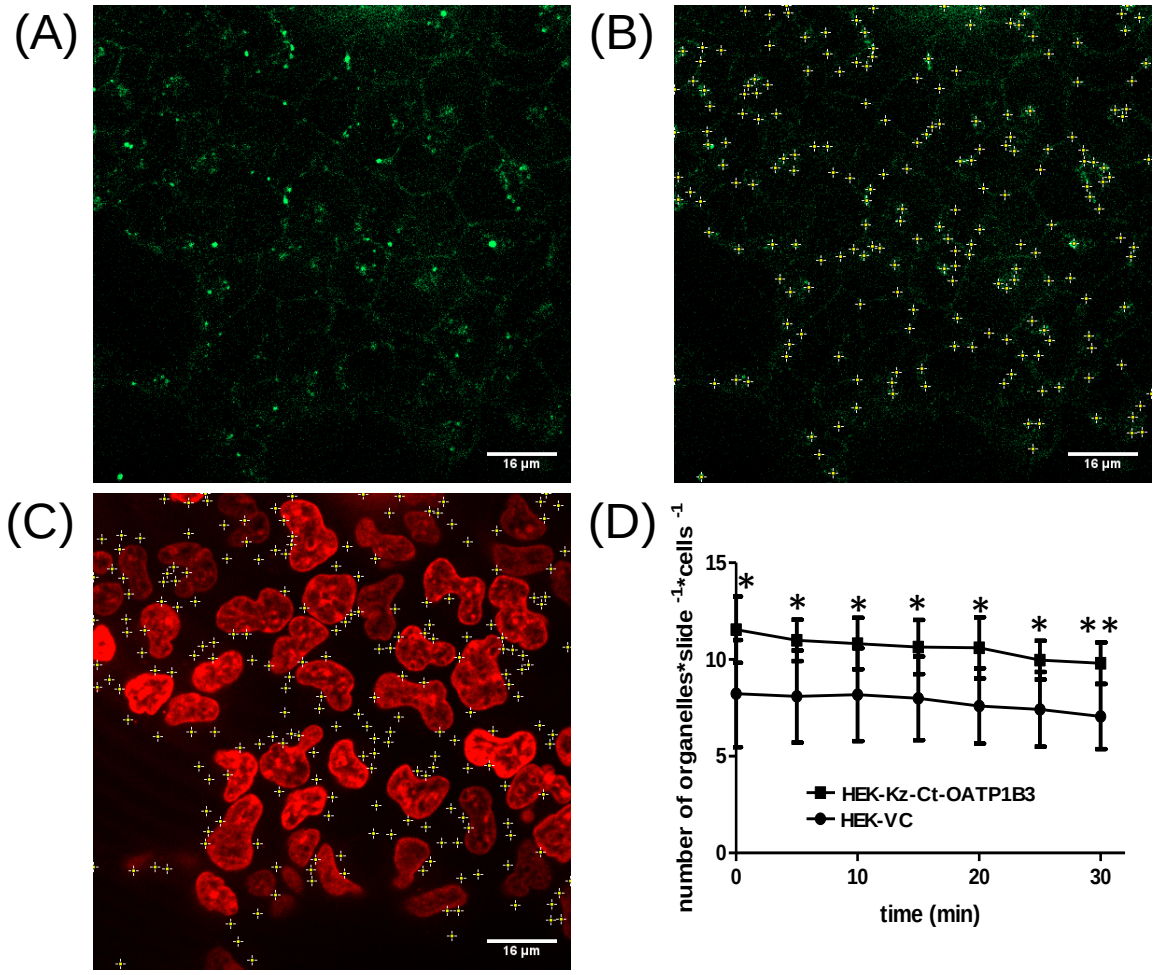

Figure S1 Quantification of stained intracellular vesicles

Cells were incubated with 1 µM OG and a 1: 1 000 dilution of SPY555-DNA. Afterwards, the cellls were analyzed via Live-cell imaging. We acquired images of five z-stacks per cell line every five minutes for 30 min (n=5). After the time exposure the stained organelles **(A)** were quantified with a software-based approach **(B)** and normalized to the number of slides and the number of nuclei **(C)**. **(D)** Comparison of the number of stained organelles in the analyzed images of HEK-VC vs. HEK-Kz-Ct-OATP1B3 cells. ** $p < 0.01$ Kz-Ct-OATP1B3 vs. VC**,** * $p < 0.05$ Kz-Ct-OATP1B3 vs. VC

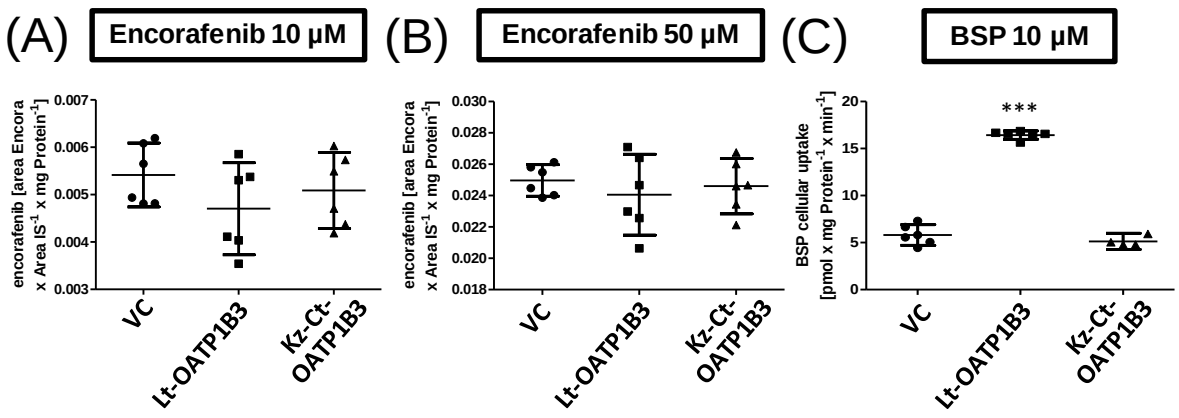

Figure S2 Cellular uptake of encorafenib

Intracellular accumulation of (A) 10 µM encorafenib and (B) 50 µM encorafenib. The area of the encorafenib peak was divided by the area of the internal standard peak and normalized to the protein. The cellular BSP uptake experiments (C) were performed on the same day as the encorafenib uptakes and served as control of the HEK-Lt-OATP1B3 transfectants. The experiments have been perfomed twice with n = 3 (n = 6) and the data are given as mean with 95 % CI. *** $p < 0.001$ Lt-OATP1B3 vs. VC, Kz-Ct-OATP1B3.

Supplemental Data: Cancer-type organic anion transporting polypeptide 1B3 (Ct-OATP1B3) is localized in lysosomes and mediates resistance against kinase inhibitors

Authors: Bastian Haberkorn , Stefan Oswald , Niklas Kehl, Arne Gessner, R. Verena Taudte, Jan Philipp Dobert , Friederike Zunke, Martin F. Fromm and Jörg König

Journal Name: Molecular Pharmacology

Manuscript: MOLPHARM-AR-2022-000539

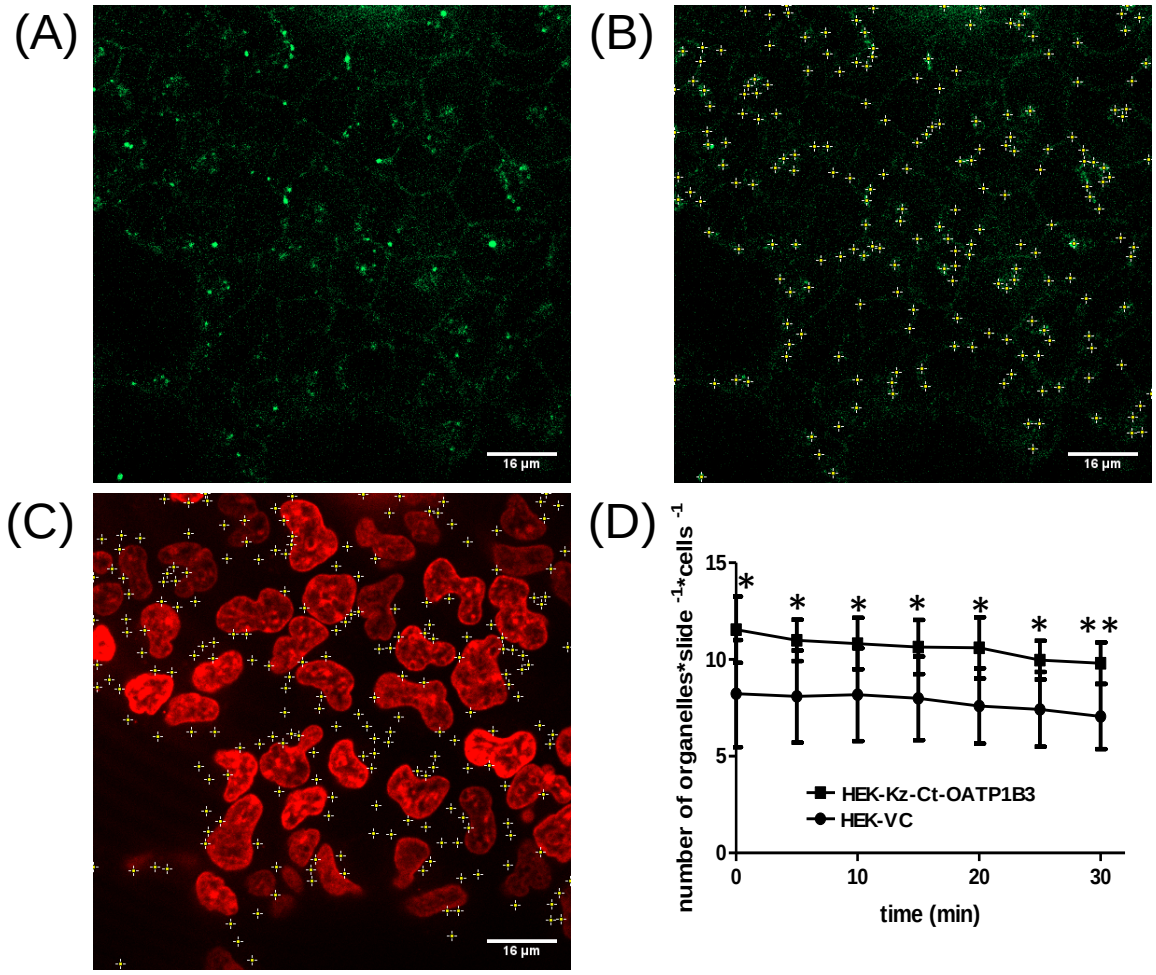

Figure S1 Quantification of stained intracellular vesicles

Cells were incubated with 1 µM OG and a 1: 1 000 dilution of SPY555-DNA. Afterwards, the cellls were analyzed via Live-cell imaging. We acquired images of five z-stacks per cell line every five minutes for 30 min (n=5). After the time exposure the stained organelles **(A)** were quantified with a software-based approach **(B)** and normalized to the number of slides and the number of nuclei **(C)**. **(D)** Comparison of the number of stained organelles in the analyzed images of HEK-VC vs. HEK-Kz-Ct-OATP1B3 cells. ** $p < 0.01$ Kz-Ct-OATP1B3 vs. VC**,** * $p < 0.05$ Kz-Ct-OATP1B3 vs. VC

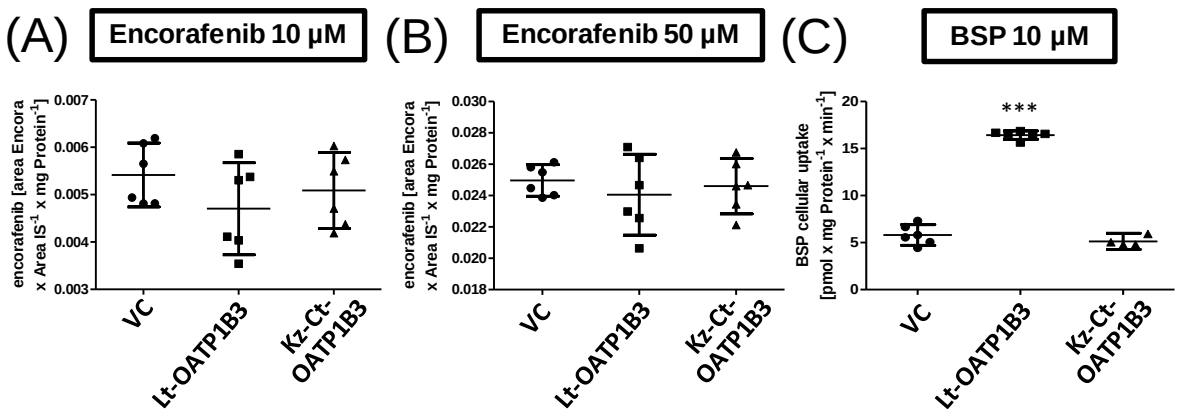

Figure S2 Cellular uptake of encorafenib

Intracellular accumulation of (A) 10 µM encorafenib and (B) 50 µM encorafenib. The area of the encorafenib peak was divided by the area of the internal standard peak and normalized to the protein. The cellular BSP uptake experiments (C) were performed on the same day as the encorafenib uptakes and served as control of the HEK-Lt-OATP1B3 transfectants. The experiments have been perfomed twice with n = 3 (n = 6) and the data are given as mean with 95 % CI. *** $p < 0.001$ Lt-OATP1B3 vs. VC, Kz-Ct-OATP1B3.